

***p*-type semiconducting properties in lithium-doped MgO single crystals**M. M. Tardío,* R. Ramírez,[†] and R. González*Departamento de Física, Escuela Politécnica Superior, Universidad Carlos III, Avda. de la Universidad, 30, 28911 Leganés, Madrid, Spain*

Y. Chen

Division of Materials Sciences, Office of Basic Energy Sciences, SC 13, U.S. Department of Energy, Germantown, Maryland 20874-1290

(Received 4 April 2002; revised manuscript received 13 June 2002; published 4 October 2002)

The phenomenally large enhancement in conductivity observed when Li-doped MgO crystals are oxidized at elevated temperatures was investigated by dc and ac electrical measurements in the temperature interval 250–673 K. The concentration of $[\text{Li}]^0$ centers (substitutional Li^+ ions each with a trapped hole) resulting from oxidation was monitored by optical absorption measurements. At low electric fields, dc measurements reveal blocking contacts. At high fields, the I - V characteristic is similar to that of a diode connected in series with the bulk resistance of the sample. Low-voltage ac measurements show that the equivalent circuit for the sample consists of the bulk resistance in series with the junction capacitance connected in parallel with a capacitance, which represents the dielectric constant of the sample. Both dc and ac experiments provide consistent values for the bulk resistance. The electrical conductivity of oxidized MgO:Li crystals increases linearly with the concentration of $[\text{Li}]^0$ centers. The conductivity is thermally activated with an activation energy of (0.70 ± 0.02) eV, which is independent of the $[\text{Li}]^0$ content. The *standard semiconducting* mechanism satisfactorily explains these results. Free holes are the main contribution to band conduction as they are released from the $[\text{Li}]^0$ -acceptor centers. In as-grown MgO:Li crystals (without $[\text{Li}]^0$ centers) the electrical current increases with time as $[\text{Li}]^0$ centers are being formed. When ample $[\text{Li}]^0$ centers are formed, an activation energy of 0.7 eV was observed. At sufficiently high current, Joule heating thermally destroys the $[\text{Li}]^0$ centers.

DOI: 10.1103/PhysRevB.66.134202

PACS number(s): 72.20.-i, 72.80.Sk, 71.38.Ht

I. INTRODUCTION

Nominally pure α - Al_2O_3 and MgO single crystals are excellent electrical insulators. At room temperature their electrical conductivities are 10^{-18} and $<10^{-20}$ $(\Omega \text{ cm})^{-1}$, respectively.^{1–3} However, a phenomenally large increase in conductivity was observed in α - Al_2O_3 and MgO crystals when doped with magnesium and lithium ions, respectively.^{3–7} In both systems hole-trapped centers are formed after oxidation at high temperatures. These centers are responsible for the electrical conductivity enhancement.^{3–7}

In virgin (as-grown) MgO:Li crystals, most of the lithium impurities are present in Li_2O precipitates.⁸ Only a small fraction, about 10^{18} cm^{-3} , are in substitutional form.⁹ These Li^+ ions are randomly distributed and are dilute. At room temperature or higher, any hole trapped by these negatively charged Li^+ sites, such as during ionizing irradiation, is unstable. Therefore there is no conductivity due to holes. On the other hand, oxidation at $T > 1100$ K disperses Li^+ ions from the precipitates such that they form “microgalaxies” containing substitutional Li^+ ions surrounding the precipitates.^{10–13} Due to the high concentration of Li^+ ions, charge neutrality requires that virtually all the substitutional Li^+ ions in the microgalaxies are each attended by a hole. These Li^+ ions are referred as $[\text{Li}]^0$ centers (a substitutional Li^+ ion with a hole trapped at one of the six oxygen nearest neighbors) and are therefore paramagnetic. It is these holes

that contribute to the *p*-type semiconductivity.

This defect absorbs light at 1.8 eV.¹² Similarly, $[\text{Mg}]^0$ centers (substitutional Mg^{2+} ions each attended by a hole) are present in oxidized α - Al_2O_3 :Mg crystals, and absorb light at 2.56 eV.^{14,15} (The nomenclature used here follows that proposed by Henderson and Wertz¹⁶ and subsequently expanded to cover other defects by Sonder and Sibley.¹⁷ The superscript refers to the net charge of the defect). In Kröger-Vink^{18,19} notation this defect is referred to as Mg_{Al}^x . Subscripts indicate the site. The effective charges (zero, negative, and positive) are indicated, respectively, by a superscript x , prime, and dot. In the $[\text{Mg}]^0$ centers, the hole is essentially confined to one lattice site, and together with the distortion it induces in the lattice is termed a small polaron.¹⁰ A *small-polaron-motion* mechanism has been proposed to explain the conductivity of Al_2O_3 :Mg crystals containing $[\text{Mg}]^0$ centers.^{5,6}

When a dc voltage was applied at ≈ 373 K to a MgO crystal containing $[\text{Li}]^0$ centers, semiconducting characteristics were observed, such as negative differential resistance, self-excited current oscillations, and avalanche breakdown.⁷ An impact ionization mechanism is responsible for these properties.⁷ In the present study, a thorough characterization of the electrical properties of MgO:Li crystals was performed in the temperature interval 250–673 K. Both ac and dc electrical measurements were made. The conductivity dependence on $[\text{Li}]^0$ concentration and temperature was investigated. The *standard semiconducting* mechanism satisfactorily explains these results.

II. EXPERIMENTAL PROCEDURE

The MgO:Li single crystals used in this study were grown by the arc-fusion technique²⁰ using a mixture of 5% Li_2CO_3 and high-purity MgO power from the Kanto Chemical Company, Japan. The concentration of lithium impurities in the resulting crystals was approximately 0.04 at.% (400 ppm). Samples with [100] faces of about 1.5 cm^2 and thickness of about 0.1 cm were obtained by cleaving and were chemically polished in hot phosphoric acid.

These samples were oxidized in flowing oxygen, at temperatures between 1223 and 1523 K, with the samples placed in a platinum basket inside an alumina tube inserted in the horizontal, axial hole of a CHESA furnace. Optical absorption measurements were performed with a Perkin-Elmer Lambda 19 spectrophotometer.

For dc measurements, voltage was applied to the crystals with a dc Sorensen DCS 150-7 voltage source. I - V characteristics were measured with an electrometer (Keithley 6512) and a voltmeter (HP 34401A). A standard three-electrical-terminal guard technique was used.²¹

For ac measurements, a function generator (Wavetek) was used, where available frequencies range from 10^{-4} to 10^7 Hz. When the sample resistance was of the order of the entrance impedance of the voltmeter, the current in the circuit was determined from the voltage drop measured in a resistor in series with the samples. Both the applied voltage and the voltage in the resistor were recorded with a voltmeter (HP 34401A). When the sample impedance is larger than $1\text{ G}\Omega$, measurements were made with an electrometer, which can measure electrical currents of 0.2 fA with $V_{\text{burden}} = 0.2\text{ mV}$. The effects of the uncompensated cables were corrected by measuring calibrated capacitances and incorporating the corrected values in the fitting function of the data.

Electrodes were made by sputtering metals with different work functions (Al, Mg, and Pt) onto two opposite lateral surfaces. Sputtering is frequently used to make contacts in electronic devices because it results in metal films with good mechanical adhesion and presumably yields ideally clean surfaces. Indium tin oxide contact (ITO) were also used. The electrical response was independent of contact electrode materials. Mostly Al electrodes were used. The temperature of the sample was monitored with a Chromel-Alumel thermocouple in direct contact with the sample.

III. EXPERIMENTAL RESULTS

To investigate the electrical conductivity of lithium-doped MgO crystals, dc and ac electrical measurements were performed on samples with different concentrations of $[\text{Li}]^0$ centers in the temperature range 250–673 K.

A. Oxidized MgO:Li crystals

1. Characterization by optical absorption spectroscopy

In MgO:Li crystals, oxidation at temperatures in excess of 1100 K produces a broad optical absorption band centered at about 1.8 eV (690 nm) due to $[\text{Li}]^0$ centers.¹² The oxidation process is very efficient in that it takes only a few minutes to

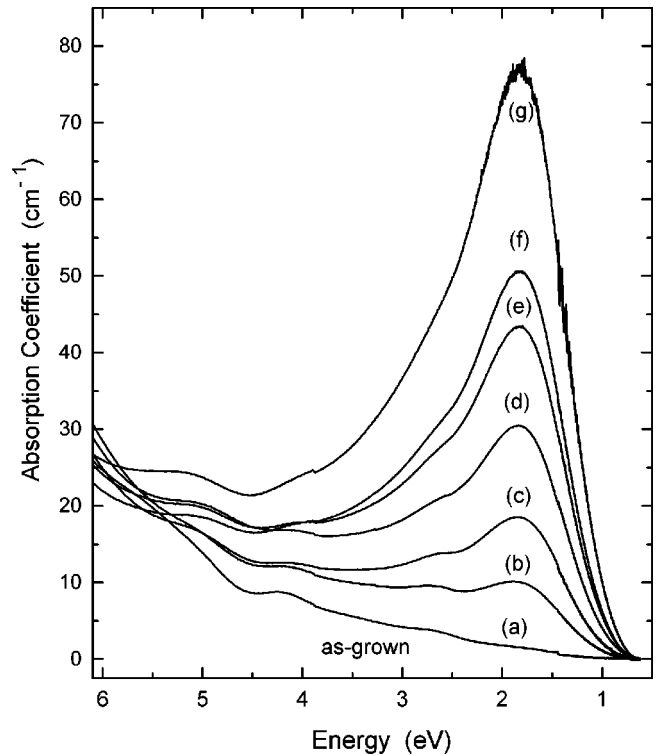


FIG. 1. Optical absorption spectra of an MgO:Li crystal (a) as-grown, and after oxidation at successively higher temperatures for 30 min at (b) 1173 K, (c) 1223 K, (d) 1273 K, (e) 1323 K, (f) 1373 K, and (g) 1473 K.

attain saturation level. Optical-absorption curves following oxidation for 30 min at increasing temperatures in the same sample are displayed in Fig. 1. The concentration of $[\text{Li}]^0$ centers can be determined⁹ from the optical-absorption coefficient, α , using Smakula's formula,

$$N = 6 \times 10^{15} f^{-1} W \alpha, \quad (1)$$

where the oscillator strength $f=0.1$ and the half-width $W = 1.44\text{ eV}$.

2. Electrical measurements

a. Direct current electrical properties. Blocking contacts are expected for hole conduction in wide band gap insulators. Sample symmetry requires that these blocking contacts are formed on both sides of the sample. In this way, regardless of the polarity of the applied voltage, one of the contacts is forwardly biased, while the other is reversely biased; on increasing the applied voltage, breakdown can occur in the reversely biased contact. For sufficiently high voltages, the overall behavior of the sample is that of an Ohmic contact with a series resistance (the bulk resistance) and a forward biased blocking contact. A typical current-voltage (I - V) characteristic is shown in Fig. 2 for a sample with a $[\text{Li}]^0$ concentration of $\approx 3.3 \times 10^{18}\text{ cm}^{-3}$. If both electrodes and their surface regions were exactly the same, the I - V characteristic would be symmetric. This characteristic is similar to that of a diode in the forward direction with a series resis-

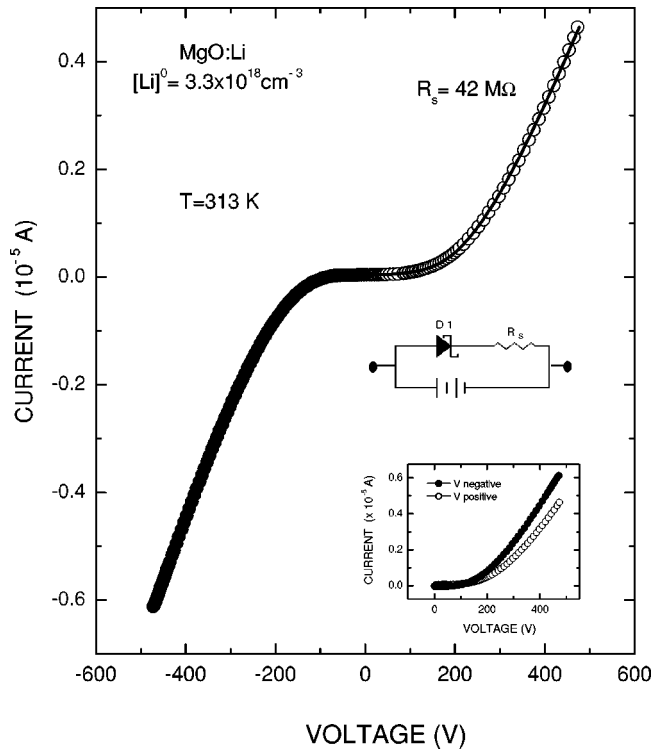


FIG. 2. Direct-current I - V characteristic at 313 K for an MgO:Li crystal containing $[\text{Li}]^0$ centers. In the inset the negative and positive parts of the curve are superimposed.

tance, R_s (the bulk resistance of the sample). The experimental points are plotted as open circles, and the solid line represents the best fit of the data to the equation

$$V = \frac{nkT}{q} \ln\left(\frac{I}{I_s} + 1\right) + IR_s, \quad (2)$$

which corresponds to a forward-biased diode in series with a resistance. Here n is the ideality factor of the junction, q is the carrier charge, and I_s is the saturation current.

For bias voltages in excess of kT/q , the current density should be proportional to $\exp(qV/kT)$. This ideal behavior is never observed in practice. Instead the current usually varies as $\exp(qV/nkT)$. The best fit was obtained when $n \gg 1$. Large n implies the existence of an interfacial layer and the recombination of electrons and holes in the depletion region. Also, the initial part of the characteristic is probably influenced by the breakdown peculiarities in the reversed direction, and consequently, the values derived for n and I_s are not fully reliable. In fact the initial part of the I - V curve can be dominated by the characteristic of the reversely biased contact; a generic exponential law for this characteristic is reasonable, which allows us to keep the same fitting equation.

The three parameters from Eq. (2) can be obtained from a fit of the experimental I - V curve: the bulk resistance R_s , the ideality factor n of the junction, and the saturation current I_s . The parameters n and I_s are affected mainly by the shape of the low-voltage part of the I - V curve. The value of the series resistance ($R_s = 42 \text{ M}\Omega$) provides a magnitude for the sample, as the ac results following this section will show, in

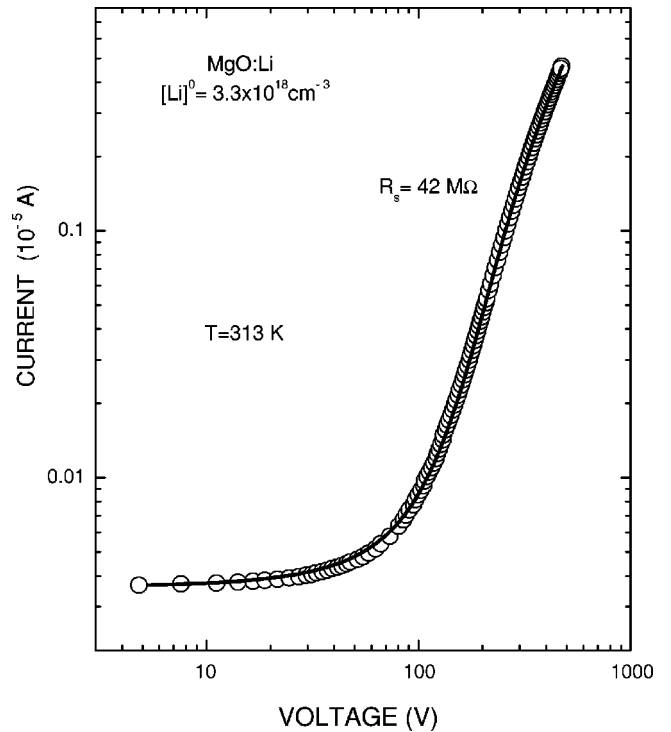


FIG. 3. Log-log plot of direct current versus voltage for the same MgO:Li crystal used in Fig. 2.

good agreement with the ac value. That this value is due to a bulk effect is supported by the fact that the same conductivity value was obtained using samples with different thicknesses and cross sections.

The Ohmic behavior at intermediate and high voltages is well illustrated in Fig. 2. The linearity of the curve at voltages higher than 250 V rules out a mechanism of space-charge-limited current, which gives a quadratic dependence of current versus voltage.²² Figure 3 shows a log-log plot of the current intensity versus voltage for the same sample used in Fig. 2. Equation (2) fits the experimental values very well.

As the temperature is raised, the bulk resistance diminishes; it is not feasible to apply the high voltages needed to break the blocking contact because of Joule dissipation in the sample. In addition, the Joule heating at currents higher than 10 mA will significantly increase the concentration of $[\text{Li}]^0$ centers formed by oxidation. For this reason the temperature range in which the Ohmic behavior can be studied is limited. Nevertheless, it is worth mentioning that the dc conductivity is thermally activated with an activation energy of $\approx 0.7 \text{ eV}$.⁷

The sample surfaces were prepared the same way, in terms of polishing procedures and applying contacts. However, the I - V curves are nonsymmetric with respect to voltage polarity (see inset, Fig. 2). This experimental asymmetry indicates that inadvertently there are still differences in the two opposite surface regions. Previous studies of thermally stimulated depolarization currents (TSD) in MgO:Li-containing $[\text{Li}]^0$ centers also reveal that the interfaces between the electrodes and the insulator are not identical for the two indium electrodes on each side of the sample.²³

As mentioned in the experimental section, for electrodes

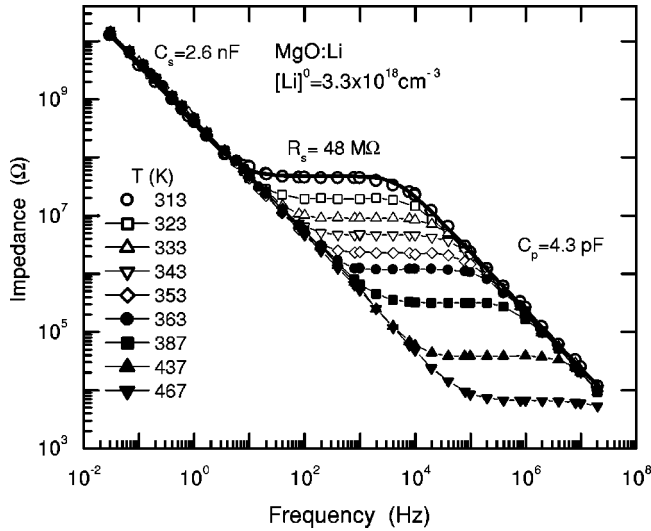


FIG. 4. Log-log plot of the impedance versus frequency for an MgO:Li crystal containing $[\text{Li}]^0$ centers. The solid line represents the best fit of the experimental points at 313 K to the equivalent circuit. The resulting values for C_s , R_s , and C_p , at this temperature are given.

we mainly used pairs of the same metal selected from Mg, Al, and Pt. Their work functions are widely different: 3.6, 4.2, and 5.6 eV, respectively. Nevertheless the electrical characteristics obtained in this study are independent of the types of metal used as electrodes. This indicates that surface effects dominate the barrier formed at the electrodes. The blocking character of the contacts has also been reported in TSD experiments.²³

In summary, dc measurements of MgO crystals containing $[\text{Li}]^0$ centers exhibit the nonlinear nature of the I - V curves. The higher-voltage regime is Ohmic and is governed by the bulk resistance of the material. The surface states are virtually nonreproducible. ac measurements complement the capacitive and resistive nature of the material and can overcome some of the difficulties encountered at the surface region.

b. Alternating current electrical properties. The experimental setup and the method of analysis of the experimental values are similar to those described in Ref. 5. The equivalent circuit for low-voltage amplitude $[(1-5)V_{\text{pk-pk}}]$ ac measurements consists of R_s in series with C_s (junction capacitance, which accounts for the blocking nature of the contacts) and in parallel with capacitance C_p , which is directly proportional to the dielectric constant of the sample. The temperature dependence of the impedance is plotted versus frequency for a sample with a $[\text{Li}]^0$ concentration of $3.3 \times 10^{18} \text{ cm}^{-3}$ (Fig. 4). The sample thickness and the electrode area were 0.10 cm and 0.52 cm², respectively. The solid line is the best fit to the equivalent circuit at 313 K. The best fit is $C_s = 2.6 \text{ nF}$, $R_s = 48 \text{ M}\Omega$, and $C_p = 4.3 \text{ pF}$ for this temperature. The dielectric constant obtained from $C_p = 4.3 \text{ pF}$ agrees with the reported values for MgO. The basic results are C_s and C_p are practically independent of temperature in the 313–467 K range, whereas the sample resistance diminishes as temperature increases. The C_s value depends

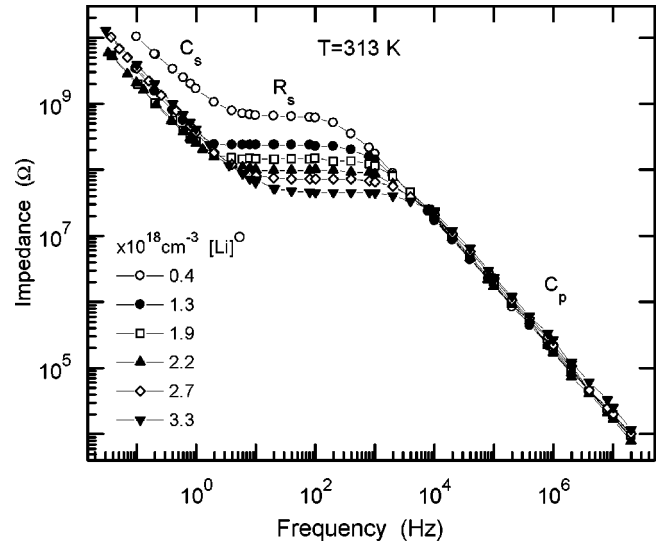


FIG. 5. Log-log plot of the impedance versus frequency for an MgO:Li crystal containing different concentrations of $[\text{Li}]^0$ centers.

on the quality of the sample surface, which we will discuss later. The data shown in Figs. 2 and 4 (open circles) were measured from the same sample; the values for R_s in both dc (42 M Ω) and ac (48 M Ω) experiments are in good agreement. At low frequencies the I - V characteristic is similar to that measured in dc.

From dc experiments using different sample geometries, we inferred that the resistance R_s determines the bulk sample conductivity, which in turn increases with $[\text{Li}]^0$ concentration. For supporting evidence, we measured the ac characteristics from different $[\text{Li}]^0$ concentrations (Fig. 5) produced in the same sample by oxidizing at progressively higher temperatures. The resistive part of the ac curve is observed to depend strongly on the $[\text{Li}]^0$ concentration. On the other hand, $C_s \approx 4.6 \text{ nF}$ and $C_p \approx 5.6 \text{ pF}$ are practically independent of the $[\text{Li}]^0$ concentration, the exception being $C_s \approx 0.7 \text{ nF}$ for the lowest concentration.

Next, we demonstrate that the conductivity is a thermally activated process involving the $[\text{Li}]^0$ center. Figure 6 shows the Arrhenius plot of the conductivity for different $[\text{Li}]^0$ concentrations in the same sample used in Fig. 5. The parallel slopes indicate the following. (1) The conductivity is thermally activated with an activation energy of $0.70 \pm 0.02 \text{ eV}$, in good agreement with previous findings.^{3,4,7} Our conductivity values agree with those reported in Ref. 4 for a sample measured at $T = 336 \text{ K}$. The results of the present work obtained at a variety of temperatures in MgO:Li crystals with different $[\text{Li}]^0$ concentrations make it possible to conclude that the conductivities are associated with a bulk conductivity effect. (2) The activation energy is independent of the $[\text{Li}]^0$ content. The dependence of the conductivity on $[\text{Li}]^0$ concentration at $T = 313 \text{ K}$ is shown in Fig. 7. These results show that there is a linear relationship between conductivity and $[\text{Li}]^0$ content. This relationship was alluded to in Ref. 3.

The effect of surface morphology was investigated. The three parameters, C_s , R_s , and C_p , were determined using one sample, which had a $[\text{Li}]^0$ concentration of 3.3

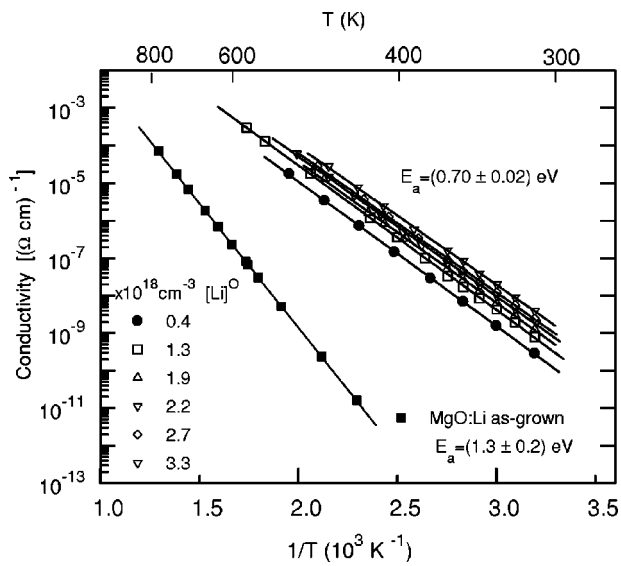


FIG. 6. Conductivity against T^{-1} for an as-grown crystal and for a crystal with different concentrations of $[Li]^0$ centers.

$\times 10^{18} \text{ cm}^{-3}$. The two faces of the sample were prepared using three distinct steps: (a) cleaved, (b) polished with diamond paste (grain size $5 \mu\text{m}$), and (c) repolished with diamond paste and etched in phosphoric acid. Following each step, magnesium electrodes were sputtered and the three pa-

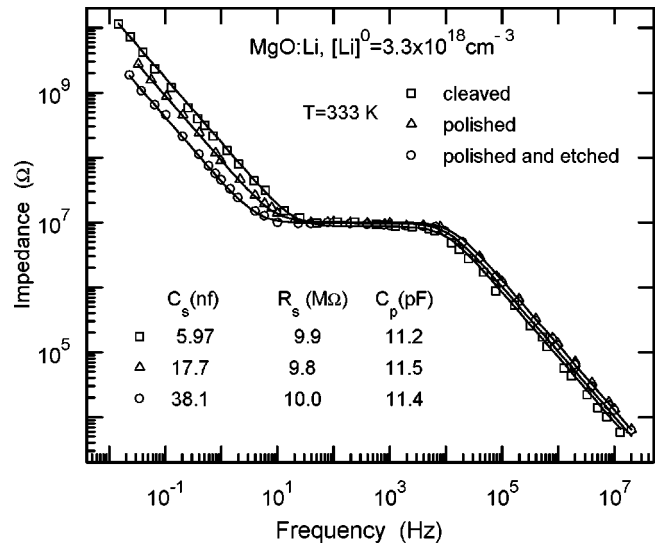


FIG. 8. Log-log plot of the impedance versus frequency at 333 K for an MgO:Li crystal containing $[Li]^0$ centers and with different surface conditions.

rameters determined. After each electrical measurement, the magnesium electrodes were removed in nitric acid before proceeding to the next step. Figure 8 shows the log-log plots of impedance versus frequency following each of the three steps. While, R_s and C_p remained constant, C_s changed sig-

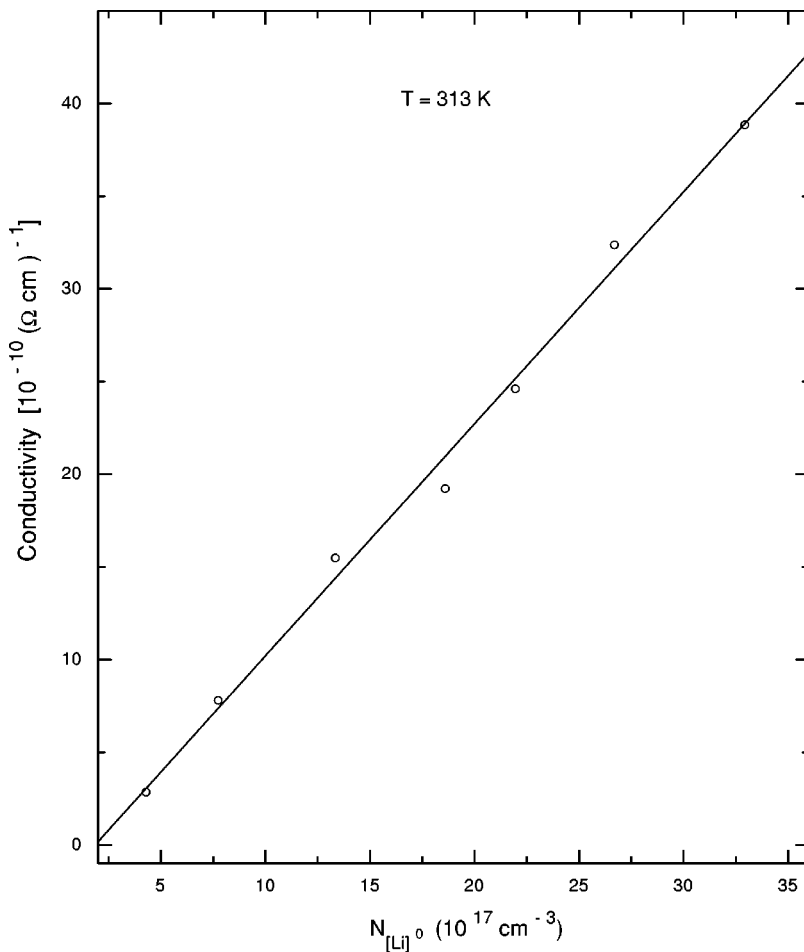


FIG. 7. Conductivity against concentration of $[Li]^0$ centers at 313 K.

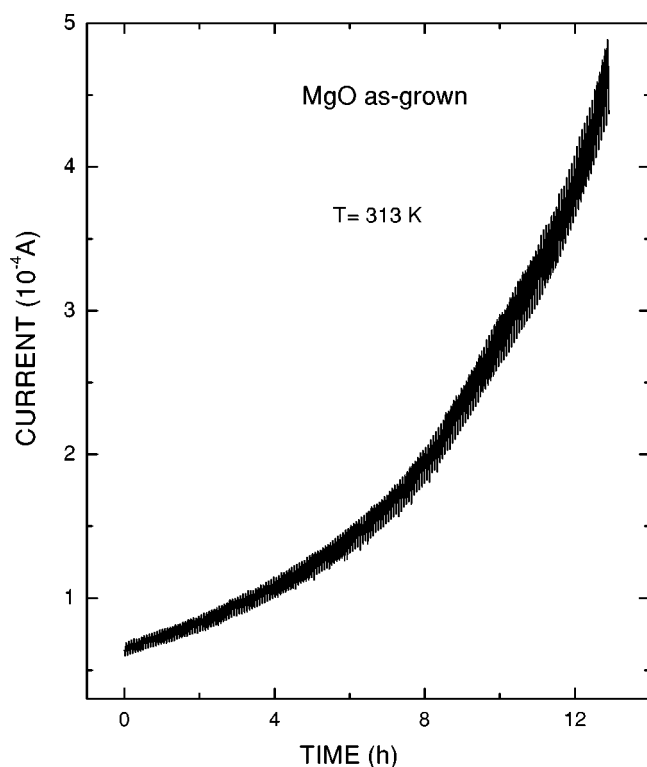


FIG. 9. Electrical current versus time for an as-grown MgO:Li crystal at 313 K.

nificantly. This result is not surprising. The first two parameters are related to the sample resistivity and to the dielectric constant of the sample, respectively, which are not affected by the quality of the sample surface. On the other hand, the junction capacitance, C_s , depends on the surface defect distribution of the Mg-MgO:Li interface. These results provide clear evidence that the random distribution of surface states controls the interface barrier. C_s must be independent of the work functions and the electron affinities of both the metal and the insulator, which are in contact. Conductive oxide electrodes, ITO, were used in an attempt to form an Ohmic contact. The results of dc and ac measurements are similar to those obtained with the metallic electrodes, which indicates that an Ohmic contact was not formed. In addition, the virtual impossibility of making an Ohmic contact in one of the electrodes makes it very difficult to characterize the barrier properties associated with the $[\text{Li}]^0$ concentration.

B. Electric-field-generated $[\text{Li}]^0$ centers

Previous studies showed that the conductivity of as-grown MgO:Li crystals to be much lower than that of oxidized crystals containing stable $[\text{Li}]^0$ centers, but much higher than that in undoped MgO crystals.²⁴ In the present work, electrical conductivity measurements were performed in virgin Li-doped MgO crystals between 400 and 800 K.

Figure 9 shows the time evolution of the current in a virgin MgO:Li sample (without $[\text{Li}]^0$ centers) at 313 K when a low electric field of 100 V/cm was applied. Initially, the current was ≈ 0.1 mA and increased slowly with time. Current oscillations were superimposed on the steady increase of

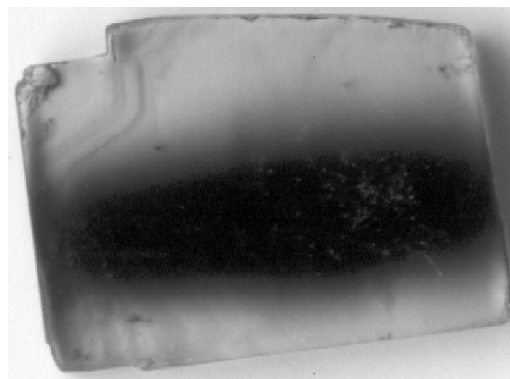


FIG. 10. Optical photograph of an MgO:Li crystal subjected to an electric field of 160 V/cm at 1373 K in vacuum for 2 min. The dark region corresponds to the area under the electrodes.

the current. These oscillations were due to oscillations of the sample temperature, with a period of about 5 min, induced by small variations in the furnace temperature; their amplitude increased as the current increased. After several hours the current increase becomes more pronounced, and given enough time, the sample experiences electrical breakdown (see Ref. 6). The current increase is attended by the emergence of *blue regions* in the area under the electrodes. Optical absorption identified the coloration as due to $[\text{Li}]^0$ centers. This observation indicates that application of an electric field creates $[\text{Li}]^0$ centers, which in turn increases the conductivity causing the current to increase and creating more $[\text{Li}]^0$ centers.

We know from the Arrhenius plots in Fig. 6 that the thermal activation energy for virgin MgO:Li crystals is 1.3 eV; when $[\text{Li}]^0$ centers are generated by oxidation at elevated temperatures, the activation energy becomes 0.70 eV. We next determine whether $[\text{Li}]^0$ centers generated by electric field yields the same activation energy. The experimental conditions are identical to those described for Fig. 9. Initially an as-grown MgO:Li crystal indeed exhibits an activation energy of 1.3 eV. After several hours of electric-field application, such that sufficient $[\text{Li}]^0$ centers were created, 0.7 eV was obtained. Activation energies between 1.3 and 0.7 eV were observed in the intermediate range.

To demonstrate visually that the characteristic blue coloration of $[\text{Li}]^0$ centers can be obtained by the application of an electric field, a virgin MgO:Li crystal was subjected to an electric field of 160 V/cm at a temperature of 1373 K for 2 min. The experiment was performed in vacuum to minimize oxygen contributions. Figure 10 shows blue coloration beneath the electrodes. Elsewhere in the sample was clear. Optical absorption indeed verified that the coloration was due to $[\text{Li}]^0$ centers.

An inverse effect can be induced by an electric field. Using an oxidized crystal, discoloration under the electrodes was observed when current exceeded 10 mA. In brief, at sufficiently high currents, Joule heating will thermally annihilate the $[\text{Li}]^0$ centers. Whether $[\text{Li}]^0$ centers are annihilated or produced in an oxidized crystal at currents higher than 10 mA is sample dependent.

IV. DISCUSSION

The results presented in previous sections show that the electrical conductivity in oxidized MgO:Li crystals increases linearly with the concentration of $[\text{Li}]^0$ centers. The conductivity is thermally activated, with an activation energy of 0.70 ± 0.02 eV, which is independent of the $[\text{Li}]^0$ content.

We shall examine three possible mechanisms to explain the thermally activated conductivity: small polaron motion,^{25,26} impurity conduction,^{27,28} or standard semiconducting behavior.²⁹ The prediction^{25,26} of the small polaron mechanism has been shown to be valid with $[\text{Mg}]^0$ centers in $\text{Al}_2\text{O}_3:\text{Mg}$ crystals.^{5,6} In spite of the similarities between $[\text{Mg}]^0$ centers in $\text{Al}_2\text{O}_3:\text{Mg}$ and $[\text{Li}]^0$ centers in MgO:Li crystals, it is unlikely that the *small-polaron motion mechanism* is responsible for the conductivity behavior in MgO:Li crystals. Although *bound* polarons were used to explain the absorption band of $[\text{Li}]^0$ centers,¹⁰ there is no compelling theoretical¹⁰ or experimental evidence to believe that *free* polarons exist in MgO. *Impurity conduction* may also be ruled out because this mechanism predicts a strong dependence of the activation energy on $[\text{Li}]^0$ concentration. Figure 6 shows that the activation energy is the same over a broad range of $[\text{Li}]^0$ centers. Hence, we are left with the *standard semiconducting mechanism*.

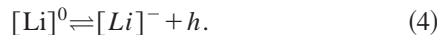
The temperature dependence of the hole conductivity ($\sigma_p = qp\mu_p$) results from the combined effect of the hole concentration, p , and the hole mobility, μ_p . The hole charge is denoted by q . The main contribution to band conduction is due to free holes from the $[\text{Li}]^0$ acceptors. The variation of the hole mobility with temperature is relatively small and depends on the scattering mechanism. This mechanism usually varies with some power of the temperature. In addition, this variation is independent of acceptor concentrations that are not excessively large, which is valid for the present experimental conditions.

The concentration of holes p is given by

$$p(T) = \frac{N_V(N_A - N_D)}{2N_D} \exp(-\phi/kT), \quad (3)$$

where N_A and N_D are the concentrations of acceptor and compensating impurities, respectively, N_V is the effective density of states in the valence band, and ϕ is the acceptor ionization energy.

The holes are created by ionization of the major neutral acceptors, $[\text{Li}]^0$ centers:



Applying the mass-action law

$$K_{[\text{Li}]^0} = \frac{N_{[\text{Li}]^-} p}{N_{[\text{Li}]^0}}, \quad (5)$$

we obtain:

$$p(T) = 2 \frac{N_{[\text{Li}]^0}}{N_{[\text{Li}]^-}} N_V \exp(-\Delta E_{[\text{Li}]^0}/kT), \quad (6)$$

where $\Delta E_{[\text{Li}]^0} = (E_{[\text{Li}]^-} - E_V)_{\text{thermal}} = 0.7$ eV, if there is no activation barrier;¹⁵ here E_V is the energy at the valence band edges.

The effective density of states in the valence band is given by²⁸

$$N_V = \left(\frac{2\pi m_p^* kT}{h^2} \right)^{3/2}, \quad (7)$$

where k is Boltzmann constant, h the Plank constant, m_p^* the effective hole mass, and T the absolute temperature. Substituting in equation (6) yields

$$p(T) = 2 \frac{N_{[\text{Li}]^0}}{N_{[\text{Li}]^-}} \left(\frac{2\pi m_p^* k}{h^2} \right)^{3/2} T^{3/2} \exp(-\Delta E_{[\text{Li}]^0}/kT). \quad (8)$$

Finally the hole conductivity σ_p is given by

$$\begin{aligned} \sigma_p(T) &= 2q \frac{N_{[\text{Li}]^0}}{N_{[\text{Li}]^-}} \left(\frac{2\pi m_p^* k}{h^2} \right)^{3/2} T^{3/2} \mu(T) \\ &\quad \times \exp(-\Delta E_{[\text{Li}]^0}/kT). \end{aligned} \quad (9)$$

This equation gives a linear dependence of the conductivity $\sigma_p(T)$ with the concentration of $[\text{Li}]^0$ in accordance with our experimental results (Fig. 7).

In addition, the $(\ln \sigma)$ versus $1/T$ curves displayed in Fig. 6 are straight lines for the temperature range (250–673 K) investigated and for different $[\text{Li}]^0$ concentrations. Our electrical measurements were made at temperatures lower than the Debye temperature of MgO ($\Xi = 743$ K). At these temperatures, $T \leq \Xi$, the scattering of holes by the lattice should be more important than the scattering by impurities, which dominates at $T \ll \Xi$. Assuming that the temperature dependence of the hole mobility is controlled by a *lattice scattering* mechanism, the hole mobility decreases with increasing temperature as $T^{-3/2}$. This results in a cancellation of the $T^{3/2}$ dependence of the carrier concentration in Eq. (8), yielding a linear relationship between $\ln \sigma$ and $1/T$. This is precisely what the results in Fig. 6 indicate. It is worth noting, however, that a temperature dependence of the preexponential term in Eq. (9) from T^{-1} to T^{-2} would produce a sufficiently small curvature in the $\ln \sigma$ vs $1/T$ curves as to go unnoticed.

V. SUMMARY AND CONCLUSIONS

Optical absorption at 1.8 eV was used to monitor the concentration of $[\text{Li}]^0$ centers in oxidized lithium-doped MgO crystals. dc and ac measurements were made to investigate the conductivity of MgO:Li samples containing different concentrations of $[\text{Li}]^0$ centers in the temperature interval 250–673 K.

At low electric fields, dc measurements reveal blocking contacts. At high fields, the I - V characteristic is similar to that of a diode with a series resistance (corresponding to a blocking contact at one side of the sample and an Ohmic contact at the other side) connected in series with the bulk resistance of the sample.

Low-voltage ac measurements reveal that the equivalent circuit for the sample consists of the bulk resistance R_s in series with C_s (the junction capacitance) connected in parallel with a capacitance C_p , which represents the dielectric constant of the bulk sample. Both dc and ac experiments provide consistent values for the bulk resistance. In the temperature interval 313–467 K, R_s decreases with increasing temperature, whereas C_s and C_p do not change significantly. The electrical conductivity of oxidized MgO:Li crystals increases linearly with the concentration of $[\text{Li}]^0$ centers. Whereas the activation energy of an as-grown MgO:Li crystal is 1.3 eV, the activation energy of a crystal containing sufficient $[\text{Li}]^0$ centers is 0.70 ± 0.02 eV, which is independent of the $[\text{Li}]^0$ content. These experimental results are in agreement with the predictions of the *standard semiconducting mechanism*. The main contribution to band conduction is due to free holes from the $[\text{Li}]^0$ centers. In spite of the similarities between MgO:Li and $\text{Al}_2\text{O}_3:\text{Mg}$ crystals, the mechanisms for hole conductivity are different: *standard semiconducting mechanism* and *small-polaron motion*, respectively.^{5,6}

When a virgin MgO:Li crystal was subjected to a low electric field of 100 V/cm, the current was observed to increase with time. Blue coloration emerged under the electrodes. Optical absorption identified the coloration as due to $[\text{Li}]^0$ centers. Temperature dependence of the conductivity showed that the activation energy decreased from 1.3 eV in the virgin state to 0.7 eV when sufficient $[\text{Li}]^0$ centers emerged.

While $[\text{Li}]^0$ centers can be created by an electric field in a virgin MgO:Li crystal, the inverse process can also be demonstrated. Using an oxidized crystal containing a large concentration of $[\text{Li}]^0$ centers, decoloration can be achieved with a sufficiently high field: the $[\text{Li}]^0$ centers are annihilated by Joule heating.

ACKNOWLEDGMENTS

Research at the University Carlos III was supported by the CICYT of Spain. The research of Y.C. is an outgrowth of past investigations performed at the Solid State Division of the Oak Ridge National Laboratory.

*Electronic address: mtardio@fis.uc3m.es

†Electronic address: ramirez@fis.uc3m.es

¹F.G. Will, H.G. deLorenzi, and K.H. Janora, *J. Am. Ceram. Soc.* **75**, 295 (1992).

²B. Evans, *J. Nucl. Mater.* **219**, 202 (1995).

³Y. Chen, R.H. Kernohan, J.L. Boldú, M.M. Abraham, D.J. Eisenberg, and J.H. Crawford, Jr., *Solid State Commun.* **33**, 441 (1980).

⁴M. Puma, A. Lorincz, J.F. Andrews, and J.H. Crawford, Jr., *J. Appl. Phys.* **53**, 4546 (1982).

⁵M. Tardío, R. Ramírez, R. González, M.R. Kokta, and Y. Chen, *Appl. Phys. Lett.* **79**, 206 (2001).

⁶M. Tardío, R. Ramírez, R. González, M.R. Kokta, and Y. Chen, *J. Appl. Phys.* **90**, 3942 (2001).

⁷R. Ramírez, R. González, R. Pareja, and Y. Chen, *Phys. Rev. B* **55**, 2413 (1997).

⁸J. Narayan, M.M. Abraham, Y. Chen, and H.T. Tohver, *Philos. Mag.* **37**, 909 (1978).

⁹Y. Chen, E. Montesa, J.L. Boldú, and M.M. Abraham, *Phys. Rev. B* **24**, 5 (1981).

¹⁰O.F. Schirmer, *Z. Phys. B* **24**, 235 (1976).

¹¹M.M. Abraham, W.P. Unruh, and Y. Chen, *Phys. Rev. B* **10**, 3540 (1974).

¹²M.M. Abraham, Y. Chen, L.A. Boatner, and R.W. Reynolds, *Phys. Rev. Lett.* **37**, 849 (1976).

¹³D.J. Eisenberg, L.S. Cain, K.H. Lee, and J.H. Crawford, Jr., *Appl. Phys. Lett.* **33**, 479 (1978).

¹⁴S.K. Mohapatra and A. Kröger, *J. Am. Ceram. Soc.* **60**, 145 (1977).

¹⁵H.A. Wang, C.H. Lee, F.A. Kröger, and R.T. Cox, *Phys. Rev. B* **27**, 3821 (1983).

¹⁶B. Henderson and J.E. Wertz, *Adv. Phys.* **17**, 749 (1968).

¹⁷E. Sonder and W. A. Sibley, in *Defects in Crystalline Solids*, edited by J.H. Crawford, Jr., and L. M. Slifkin (Plenum, New York, 1972).

¹⁸F.A. Kröger and H.J. Vink, in *Solid State Physics*, edited by F. Seitz and D. Turnbull, (Academic, New York, 1956), Vol. 3, p. 307.

¹⁹F.A. Kröger, *The Chemistry of Imperfect Crystals* (North-Holland, Amsterdam, 1974), Vol. 2, p. 14.

²⁰M.M. Abraham, C.T. Butler, and Y. Chen, *J. Chem. Phys.* **55**, 3757 (1976).

²¹R. M. Blumenthal M.A. Seitz, in *Electrical Conductivity in Ceramics and Glass*, edited by N.M. Tallan (Dekker, New York, 1979), Part A, p. 101.

²²N.F. Mott and R.W. Gurney, *Electronic Processes in Ionic Crystals* (Dover, New York, 1964).

²³R. Vila, A. Ibarra, M. Jiménez de Castro, and Mariani, *Solid State Commun.* **90**, 61 (1994).

²⁴R. Ramírez, R. González, R. Pareja, and Y. Chen, *Mater. Sci. Forum* **41**, 239 (1997).

²⁵D. Emin and T. Holstein, *Ann. Phys. (N.Y.)* **53**, 439 (1969).

²⁶H. Frölich, *Adv. Phys.* **54**, 325 (1954).

²⁷M. Pollak and T.H. Geballe, *Phys. Rev.* **122**, 1742 (1961).

²⁸K. Seeger, *Semiconductor Physics* (Springer, Berlin, 1989), p. 34–51.

²⁹I. Freidman and T. Holstein, *Ann. Phys. (N.Y.)* **21**, 494 (1963).